

# Multifractal Texture Analysis using a Dilation-based Hölder Exponent

Joao Batista Florindo<sup>1</sup>, Odemir Martinez Bruno<sup>2</sup> and Gabriel Landini<sup>1</sup>

<sup>1</sup>College of Medical and Dental Sciences, University of Birmingham, St Chad's Queensway, Birmingham, U.K.

<sup>2</sup>Physics Institute of Sao Carlos, University of Sao Carlos, Sao Carlos, Brazil

**Keywords:** Multifractal, Texture Classification, Bouligand-Minkowski, Fractal Geometry.

**Abstract:** We present an approach to extract descriptors for the analysis of grey-level textures in images. Similarly to the classical multifractal analysis, the method subdivides the texture into regions according to a local Hölder exponent and computes the fractal dimension of each subset. However, instead of estimating such exponents (by means of the mass-radius relation, wavelet leaders, etc.) we propose using a local version of Bouligand-Minkowski dimension. At each pixel in the image, this approach provides a scaling relation which fits better to what is expected from a multifractal model than the direct use of the density function. The performance of the classification power of the descriptors obtained with this method was tested on the Brodatz image database and compared to other previously published methods used for texture classification. Our method outperforms other approaches confirming its potential for texture analysis.

## 1 INTRODUCTION

Since the seminal work of Julesz (Julesz, 1981), the analysis of texture images, and particularly texture classification, have played a fundamental role in many applications such as remote sensing, image retrieval, object recognition, and others (Zhang and Tan, 2002). Methods such as textons (Varma and Zisserman, 2009), texels (Todorovic and Ahuja, 2009), density maps (Ardizzone et al., 2013) and several others have been particularly successful in the solution of highly complex problems (Farinella et al., 2014).

Among the methods of texture analysis, model-based approaches (Materka and Strzelecki, 1998) are especially flexible to analyse a large variety of images, since they are constructed over adaptable parameters. One of the model-based methods that provided interesting results in texture classification is based on the use of the multifractal spectrum (Xu et al., 2009). That approach is not only precise in enabling discrimination between different images but it is also robust to some changes in illumination and viewpoint. Despite this, the method relies on local Hölder exponents obtained by applying a Gaussian convolution to the pixel neighbourhood, suggesting that more elaborated approaches might be helpful to describe textures.

Here we propose to use a local Hölder exponent based on the measure of Bouligand-Minkowski dila-

tion volumes. That approach has shown to provide efficient texture characterisation via the “fractal descriptors” (Florindo and Bruno, 2013) and may provide a more precise representation of local textures in terms of irregularity. In this context, the local dimension is estimated by mapping the pixels within a local neighbourhood into a cloud of points in a three-dimensional space. Therefore, each point in this cloud is progressively dilated by spheres with growing radius and the local Hölder exponent is computed from the exponential relation between the radius of the spheres and the volume of the dilated cloud.

We applied this approach to the classification of 40 classes from the Brodatz images database (Brodatz, 1966) and the task performance was compared to other state-of-the-art and classical descriptors previously published in the literature. The potential of this modified version of the local dimension is demonstrated by the ratio of images correctly classified in the database, which was higher than with the other reported methods.

## 2 FRACTAL GEOMETRY

Fractal Geometry was developed from the mid seventies by Mandelbrot (Mandelbrot, 1982) to provide a means to characterise objects which could not be described accurately by means of Euclidean Geometry.

Many natural structures are irregular and despite that natural objects are not strictly fractals in a mathematical sense (e.g. they are not infinitely detailed), they have, nevertheless, characteristics that suggest that they are better modelled by Fractal Geometry concepts (such as their complexity and self-similarity) at least within a limited interval of scales.

The most widely used measure of an object in Fractal Geometry is the fractal dimension and one of its mathematical definitions is called Hausdorff-Besicovitch dimension, formally defined by:

$$D(E) = \lim_{\delta \rightarrow 0} \frac{N(\delta, E)}{\log \delta}, \quad (1)$$

where  $N(\delta, E)$  is the minimum number of sets with diameter  $\delta$  necessary to cover  $E$ . For real-world objects the definition of an infinite covering is not feasible and several approximations for  $N(\delta, E)$  have been proposed in the literature (Falconer, 2003), such as box-counting, Bouligand-Minkowski dilation, mass-radius relation, and so on.

### 3 MULTIFRACTALS

Multifractal theory assumes that certain class of objects (multifractals) have different degrees of self-similarity in different sub-parts and therefore they should be approximated by several fractal-like modellings (with different fractal dimensions) instead of using only one global dimensional value.

The analysis is performed in a few steps. First, the image is divided into local subsets, then the scaling of a measure in this subsets (i.e. the local Hölder exponent  $\alpha$ ) is computed. Finally, the fractal dimensions  $f(\alpha)$  of the sets of locations with local Hölder exponent  $\alpha$  is computed. That relation of values is the multifractal spectrum of the image and can be used as descriptors of the image texture.

Whereas there are different approaches to obtain the multifractal spectrum, here we focus on the solution proposed in (Xu et al., 2009) because it is straightforward in implementation, it achieved good results in texture classification and showed to be relatively invariant to certain scale and illumination changes.

The local measure  $\mu$  employed in (Xu et al., 2009) is named “density function” and it is defined at each point  $p$  in an intensity image  $I$  by

$$\mu(p) = \int \int_{B(p,r)} (G_r * I) dp, \quad (2)$$

where  $B(p, r)$  is a disk centred at  $p$ , with radius  $r$ , and

$G_r$  is a circular Gaussian kernel with radius  $r$ :

$$G_r = \frac{1}{r\sigma\sqrt{2\pi}} e^{-\frac{\|p\|^2}{2\sigma^2 r^2}}, \quad (3)$$

for some smoothing parameter  $\sigma$ . The Hölder exponent is computed by

$$\alpha(p) = \lim_{r \rightarrow 0} \frac{\log \mu(B(p, r))}{\log r}. \quad (4)$$

The limit is estimated from the slope of a straight line fit to the curve of  $\log r \times \log \mu(B(p, r))$ .

Secondly, the computation of the multifractal spectrum (MFS), is achieved by dividing the image into subsets  $E_k$  according to

$$E_k = \{p \in \mathfrak{R}^2 : \alpha(p) = k\} \quad (5)$$

and computing the respective fractal dimension  $D$ , such that the MFS is obtained by:

$$MFS = \{D(E_k) : k \in \mathfrak{R}\}, \quad (6)$$

where  $D$  can be computed by Equation 1.

### 4 PROPOSED METHOD

The dividing process makes possible to think of multifractal analysis as an elaborated histogram of the image, where the homogeneity of the texture is assessed under two perspectives: one local, given by the Hölder exponent and one global, provided by the fractal dimensions of each subset resulting from the division of the image. As consequence, the local Hölder exponent plays a fundamental role in the analysis and therefore should be carefully defined.

The neighbourhood value  $\alpha(p)$ , which in (Xu et al., 2009) is computed via the density function  $\mu(B(p, r))$ , is an example of a Hölder exponent (Bedford, 1989). Such parameter is more generically defined in the context of Hölder condition. A function  $f$  satisfies this condition if, for any  $x$  and  $y$  in its domain, the following inequality holds:

$$|f(x) - f(y)| \leq C \|x - y\|^\alpha, \quad (7)$$

where  $C$  is a real constant and  $\alpha$  is the Hölder exponent. An especially interesting case occurs when  $\alpha = 1$ , and the function is said to be Lipschitz-invariant. This is a key property in the theory of multifractals because it assures the local invariance often desired in image analysis. The density function is an example of this category but some other functions invariant under self-affine transforms could be employed.

Based on this assumption, here, a local Hölder exponent based on the Bouligand-Minkowski dilations

is proposed. Similarly to  $\alpha(p)$  the new exponent hereafter called  $\beta(p)$  is parametrized by the size  $r$  of the neighbourhood. At each point  $p \in I$ , with coordinate  $(i, j)$ , a window  $w : I([i-r, i+r], [j-r, j+r])$  is extracted and mapped onto a cloud of points  $\mathcal{C}(w)$ , satisfying:

$$(i, j, k) \in \mathcal{C}(w) \leftrightarrow w(i, j) = k. \quad (8)$$

In the following, each point  $p \in \mathcal{C}(w)$  is dilated by a sphere  $B(p, d)$ , centred at  $p$  with radius  $d$  and the dilated volume is computed through

$$V(d) = \bigcup_{p \in \mathcal{C}(w)} B(p, d). \quad (9)$$

The local Hölder exponent  $\beta(p)$  is computed by

$$\beta(p) = \lim_{d \rightarrow 0} \frac{\log V(d)}{\log d}, \quad (10)$$

and this limit is estimated by fitting a straight line to the curve  $\log d \times \log V(d)$  and computing the corresponding slope for each point in the image. Finally, the exponent is locally assigned to the pixel  $p$ . Figure 1 illustrates the steps involved in the dilation process of the pixels within  $w$ .

In order to verify how well  $\beta(p)$  estimates the Hölder exponent and consequently the multifractal spectrum of a grey-level image, Figure 2 compares the proposed  $f(\beta)$  with the method in (Xu et al., 2009) over a synthetic multifractal texture. Figure 2(a) shows the image generated by the Meakin model (Meakin, 1987). Figure 2(b) exhibits  $f(\alpha)$  curve obtained through (Xu et al., 2009) and the proposed one compared to the theoretical spectrum, obtained by a procedure described in (Chhabra et al., 1989). Figure 2(c) shows a histogram of the average error when fitting a straight line to the log – log curve at each point  $p$ .

The  $f(\alpha)$  and  $f(\beta)$  curves have a similar shape to that of the expected curve, although the experimental values obtained depart from the theoretical values, due to the data being a discrete image. In the particular case of  $f(\beta)$  this is also caused by the sparsity of the spheres in the space. An isolated point that is dilated and suddenly becomes connected to other dilated points has its volume raised very quickly leading to overestimated values of the exponent. However, the  $\log d \times \log V(d)$  curve in the proposed method showed the best fit to a straight line than  $\log \mu(B(p, r)) \times \log r$  in (Xu et al., 2009), as illustrated by the smaller error in the histogram. Such behaviour is due largely to the smoother growing of the dilation volume when the radius is gradually increased.

Finally, Figure 3 illustrates the obtained Hölder exponents for a texture of example from the real-world and the respective multifractal spectrum. Here,

even the shape of the spectrum curve is different from those found in well-defined multifractals like in the Meakin model, which again can be explained by the limited number of scales allowed by the image domain. Another important remark here is that the values of  $\alpha$  (or  $\beta$ ) are expected to stay between 2 and 3, since they are basically the fractal dimension of an object immersed in the three-dimensional topological space. However, here the sparsity of spheres in more discontinuous regions of the image causes the exponent to extrapolate such interval, as previously explained. Such extrapolation is also common in other applied works on multifractals, like (Xu et al., 2009; Meakin, 1987; Bedford, 1989) and several others.

Following (Xu et al., 2009), this exponent is also computed not only on the intensity image, but on the image gradient, and on its Laplacian. Therefore, three variants of  $\beta(p)$  are defined:

$$\beta_I(p) = \lim_{d \rightarrow 0} \frac{\log \bigcup_{p \in \mathcal{C}(w)} B(p, d)}{\log d}, \quad (11)$$

$$\beta_G(p) = \lim_{d \rightarrow 0} \frac{\log \bigcup_{p \in \mathcal{C}(\nabla w)} B(p, d)}{\log d}, \quad (12)$$

and

$$\beta_L(p) = \lim_{d \rightarrow 0} \frac{\log \bigcup_{p \in \mathcal{C}(\nabla^2 w)} B(p, d)}{\log d}, \quad (13)$$

From equations 5 and 6, three MFS vectors are obtained ( $M_I^\beta$ ,  $M_G^\beta$  and  $M_L^\beta$ ) and they are concatenated to be used as the texture descriptors. The descriptors based on  $\beta(p)$  were also interchanged and merged with those from  $\alpha(p)$  to obtain even more precise classification.

## 5 EXPERIMENTS

Some parameters in the proposed method were empirically chosen. Thus to estimate the Hölder exponent by the Bouligand-Minkowski method a maximum dilation radius of 5 and a  $5 \times 5$  neighbourhood were employed at each pixel. Moreover, the values of  $\beta$  were limited within the interval  $[1, 4]$  and sampled into 33 bins, so that each  $M_I^\beta$ ,  $M_G^\beta$  and  $M_L^\beta$  is a vector of 33 real values.

The proposed method was used for the classification of Brodatz textures (Brodatz, 1966). The first 40 images (D1-D40) at a resolution of 512x512 pixels were used. All images were divided into 16 non-overlapping windows giving rise to a final set of 40 classes with 16 images in each class. The Brodatz collection is made of a set of texture images containing a wide variety of levels of regularity, granularity,

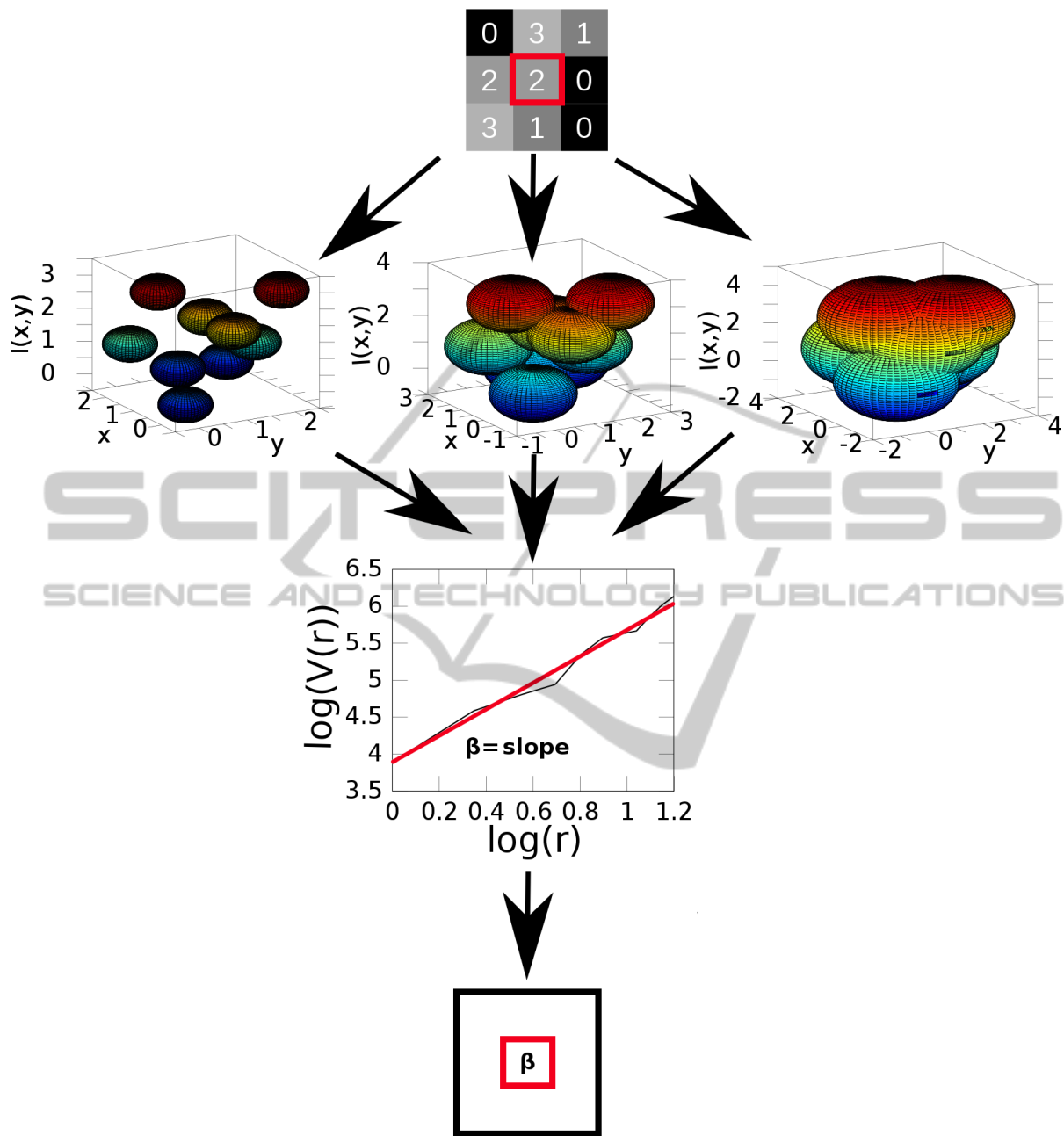


Figure 1: A simplified  $3 \times 3$  texture image, the cloud being dilated by variable radius and the slope of the log – log curve used to estimate the Hölder exponent. Such exponent is locally assigned to the central pixel. The dilation is shown as being continuous only for illustration purposes.

periodicity and scale, making it ideal for image classification benchmarking purposes, specially with multiscale approaches such as the method presented here.

The performance of the proposed descriptors as classifiers was compared to other previous work using Local Binary Patterns (LBP) (Ojala et al., 1996), Grey-Level Co-occurrence Matrix (GLCM) (Haralick, 1979), the multifractal approach in (Xu et al.,

2009), Fourier (Gonzalez and Woods, 2002) and fractal descriptors (Backes et al., 2009). To allow for fair comparisons and to reduce the internal correlations all the descriptors were submitted to a Principal Component Analysis (PCA) (Duda and Hart, 1973) for dimensionality reduction.

Finally, the classification was carried out by Linear Discriminant Analysis (LDA) (Duda and Hart,

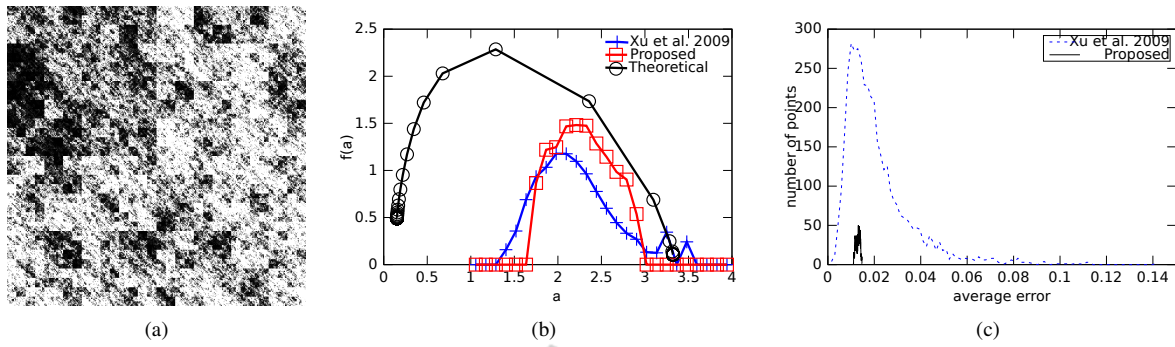


Figure 2: Multifractal analysis of a synthesized multifractal image. (a) Grey-level multifractal image generated by the procedure described in (Meakin, 1987). (b)  $f(\alpha)$  curves comparing the proposed method to that in (Xu et al., 2009) and the expected theoretical curve provided by the method in (Chhabra et al., 1989). (c) Histogram of the average error in the log – log fitting at each point of the image.

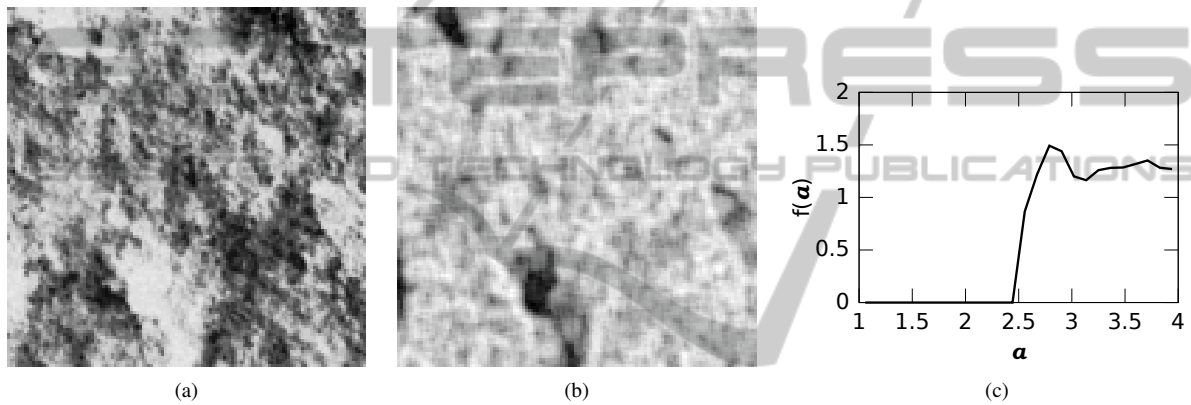


Figure 3: Multifractal analysis of a real-world texture. (a) Original image (sample c002\_002 from Brodatz database (Brodatz, 1966)). (b) Local dilation-based Hölder exponent. (c) Multifractal spectrum.

1973), following a 10-fold scheme, that is, the database was split into 10 groups of equal sizes and 10 rounds of classification were executed. In each round, 9 groups were used to train and the remaining one to test. The final correctness rate is given by the average correctness over all the rounds.

## 6 RESULTS AND DISCUSSION

Table 1 shows the correctness rates achieved during the classification process when using different combinations of MFS vectors, either using the original  $\alpha(p)$  Hölder exponent or the proposed  $\beta(p)$  value. From the table it can be observed that  $M^\beta$  performs better on the intensity and on the gradient of the image rather than on the Laplacian. Besides, a higher percentage of the images (95.78%) was correctly discriminated when  $M^\alpha$  and  $M^\beta$  descriptors were combined through the PCA technique.

Table 2 compares the best combination in Table 1

with other texture descriptors widely used in the literature. The proposed approach correctly classified a larger number of images even outperforming methods whose efficiency in this task is well established. Such result is consequence of using a richer local description of the texture, yielding to more meaningful multifractal spectra

Figure 4 exhibits the confusion matrices for the method as originally proposed in (Xu et al., 2009) together with the approach here proposed. In this type of representation a minimum of light blue points outside the diagonal is expected and, although the difference is not so clear, the proposed descriptors presents fewer misclassification over the classes.

The method in its current version also presents a drawback which is the high computational time involved since the dimension is computed at each pixel ( $O(N^2)$  for an  $N \times N$  image), although this is attenuated by using optimized algorithms as those used in (Backes et al., 2009). Anyway this computational time should be improved in the future by means of

Table 1: Correctness rate obtained by combining  $\alpha$  and  $\beta$  in different ways.

Name	Combination	Correctness rate (%)
MFS1	$M_I^\beta$	70.00
MFS2	$M_G^\beta$	80.94
MFS3	$M_L^\beta$	57.66
MFS4	$M_I^\beta + M_G^\beta + M_L^\beta$	89.06
MFS5	$M_I^\alpha + M_G^\alpha + M_L^\alpha + M_I^\beta + M_G^\beta + M_L^\beta$	95.00
MFS6	$M_I^\alpha + M_G^\alpha + M_L^\alpha + M_I^\beta + M_G^\beta$	95.78

Table 2: Correctness rate and respective cross-validation errors obtained by the compared descriptors.

Method	Correctness rate (%)	Error
Fourier	88.75	0.05
GLCM	91.67	0.04
Fractal Descriptors	94.37	0.03
LBP	95.00	0.04
(Xu et al., 2009)	93.75	0.05
Proposed MFS6	95.78	0.03

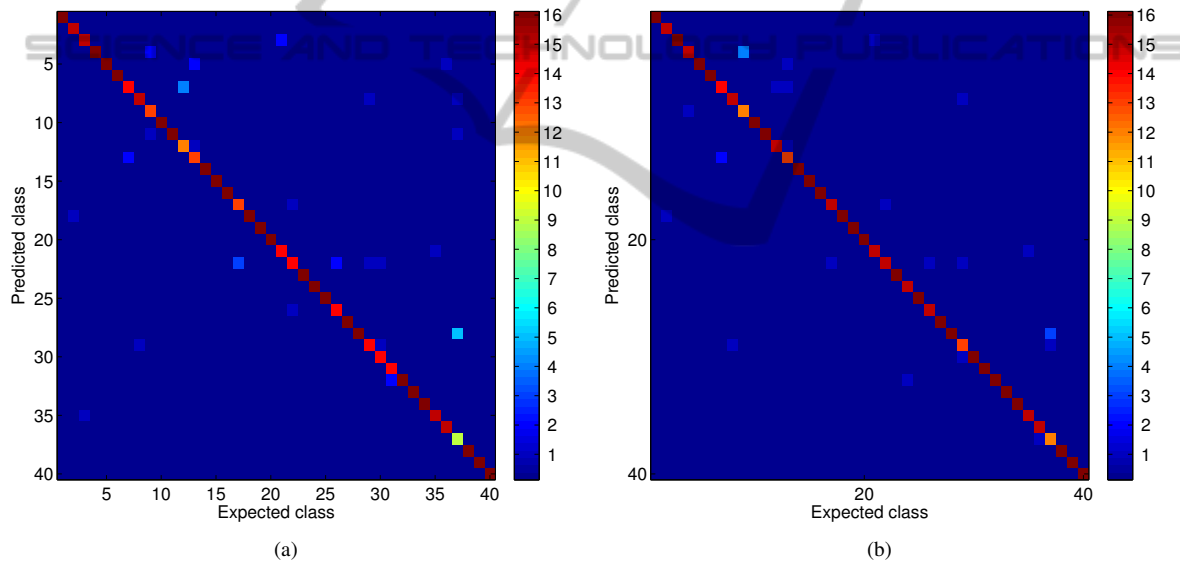


Figure 4: Confusion matrices. (a) (Xu et al., 2009). (b) Proposed.

a more parallelized procedure. Another point is that PCA is a simple approach and more advanced feature selection algorithms also can be applied providing even better results.

Generally speaking,  $M^\beta$  descriptors enhanced the classification performance of the multifractal analysis and added meaningful information to  $M^\alpha$  descriptors, such that when they are combined more images are correctly classified. Nevertheless, the proposed Hölder exponent did not succeed when applied over the Laplacian of the image. Such behaviour can be explained by the dilation process, which propagates the discontinuities on this type of image and makes

the local exponent more unstable than the smoothing effect of the Gaussian convolution in (Xu et al., 2009).

## 7 CONCLUSIONS

We presented a method to estimate the local Hölder exponent in grey-level images and applied it in the division step of the multifractal analysis of these images. Our approach is an adaptation of the Bouligand-Minkowski fractal dimension analysis, here computed over the neighbourhood of pixels. It was introduced into the pipeline of the multifractal process and com-

puted over the intensity grey-level image as well as over the gradient and the Laplacian of the same image.

The efficiency of the proposed approach was tested in the classification of 40 classes of Brodatz database, and compared to other classical texture descriptors and the multifractal approach described in (Xu et al., 2009). The results showed that the new descriptors can be combined to the previous multifractal analysis and in this way they are capable of outperforming the classification results of other state-of-the-art methods in the literature.

Such promising results suggest that the dilation process successfully employed in a multiscale description of textures can also be a reliable method to locally characterize a neighbourhood providing meaningful descriptors in the context of a multifractal analysis.

## ACKNOWLEDGEMENTS

Joao Batista Florindo acknowledges support from FAPESP (The State of São Paulo Research Foundation) (Grant No. 2013/22205-3). Odemir Martinez Bruno acknowledges support from CNPq (National Council for Scientific and Technological Development, Brazil) (Grant Nos. 484312/2013 and 308449/2010).

## REFERENCES

- Ardizzone, E., Bruno, A., and Mazzola, G. (2013). Scale detection via keypoint density maps in regular or near-regular textures. *Pattern Recognition Letters*, 34(16):2071–2078.
- Backes, A. R., Casanova, D., and Bruno, O. M. (2009). Plant leaf identification based on volumetric fractal dimension. *International Journal of Pattern Recognition and Artificial Intelligence*, 23(6):1145–1160.
- Bedford, T. (1989). Hölder exponents and box dimension for self-affine fractal functions. *Constructive Approximation*, 5(1):33–48.
- Brodatz, P. (1966). *Textures: A photographic album for artists and designers*. Dover Publications, New York.
- Chhabra, A., Meneveau, C., Jensen, R., and Sreenivasan, K. R. (1989). Direct determination of the  $f(\alpha)$  singularity spectrum and its application to fully developed turbulence. *Physical Review A*, 40(9):5284–5294.
- Duda, R. O. and Hart, P. E. (1973). *Pattern Classification and Scene Analysis*. Wiley, New York.
- Falconer, K. (2003). *Fractal Geometry: Mathematical Foundations and Applications*. Wiley, Chichester, UK.
- Farinella, G. M., Allegra, D., and Stanco, F. (2014). A benchmark dataset to study the representation of food images. In *International Workshop on Assistive Computer Vision and Robotics (ACVR)*.
- Florindo, J. B. and Bruno, O. M. (2013). Texture analysis by multi-resolution fractal descriptors. *Expert Systems with Applications*, 40(10):4022–4028.
- Gonzalez, R. C. and Woods, R. E. (2002). *Digital Image Processing (2nd Edition)*. Prentice Hall, Upper Saddle River.
- Haralick, R. M. (1979). Statistical and structural approaches to texture. *Proceedings of the IEEE*, 67(5):786–804.
- Julesz, B. (1981). Textons, the elements of texture perception, and their interactions. *Nature*, 290(5802):91–97.
- Mandelbrot, B. B. (1982). *The Fractal Geometry of Nature*. Freeman.
- Materka, A. and Strzelecki, M. (1998). Texture analysis methods – a review. Technical report, Institute of Electronics, Technical University of Lodz.
- Meakin, P. (1987). Random walks on multifractal lattices. *Journal of Physics A: Mathematical and General*, 20(12):L771.
- Ojala, T., Pietikäinen, M., and Harwood, D. (1996). A comparative study of texture measures with classification based on featured distributions. *Pattern Recognition*, 29(1):51–59.
- Todorovic, S. and Ahuja, N. (2009). Texel-based texture segmentation. In *ICCV*, pages 841–848. IEEE.
- Varma, M. and Zisserman, A. (2009). A statistical approach to material classification using image patch exemplars. *IEEE Transactions on Pattern Analysis and Machine Intelligence*, 31(11):2032–2047.
- Xu, Y., Ji, H., and Fermüller, C. (2009). Viewpoint invariant texture description using fractal analysis. *International Journal of Computer Vision*, 83(1):85–100.
- Zhang, J. and Tan, T. (2002). Brief review of invariant texture analysis methods. *Pattern Recognition*, 35(3):735–747.